Electronic supplementary information (ESI)

Development of a Boron-Doping Strategy to Activate Luminescence in a Non-Emissive Silver-Incorporated Polyoxoniobate

Li-Hao Hong,† De-Qing Qian,† Yan-Jia Lin, Sheng-nan Yue, Xing Huang, Hao-Hong Li*, Xin-Xiong Li*, and Shou-Tian Zheng*

Fujian Provincial Key Laboratory of Advanced Inorganic Oxygenated Materials, State Key Laboratory of Photocatalysis on Energy and Environment, College of Chemistry, Fuzhou University, Fuzhou, Fujian 350108, China
E-mail: *lihh@fzu.edu.cn; lxx@fzu.edu.cn; stzheng@fzu.edu.cn.*

Section S1 Experimental section

S1.1 Measurements and Materials

Except that $K_7H[Nb_6O_{19}]\cdot 13H_2O$ precursor was prepared as described in the literature,[1] Boronic acid of chemical purity grade was sourced from Sinopharm (China National Pharmaceutical Group)，other chemicals were commercially purchased and directly used without further purification. IR spectra of all compounds were determined in the range of 4000−500 cm^{-1} on a Nicolet IS50 Fourier transform infrared (FT/IR) spectrometer. Powder X-ray diffraction (PXRD) patterns were obtained using an Ultima IV diffractometer with Cu Kα radiation (λ = 1.5418 Å) in the range of 5−50°. UV-vis spectra were performed on a SHIMADZU UV-2600 UV-visible spectrophotometer by using $BaSO_4$ as the blank. Steady-state emission and transient fluorescence spectra were acquired using Edinburgh Instruments FLS980 spectrometer. The test was conducted using the FLS1000 steady-state/transient fluorescence spectrometer from Edinburgh Company. The absolute photoluminescence quantum yield was measured using the FLS1000 spectrometer from Edinburgh Instruments, UK. The absolute quantum yield was determined by the N-M01 integrating sphere accessory from Shanghai Tianmei Scientific Instrument Co., LTD. The test conditions are as follows: A 450 W ozone-free xenon lamp was used as the light source. Under the excitation of 365 nm wavelength, the spectrum was scanned in the range of 340 to 800 nm. The slit widths of the excitation and emission monochromators were set at 4.30 nm and 0.43 nm respectively, and a photomultiplier tube was used for detection. The systematic error of this measurement was controlled within ±0.5%. XPS (X-ray photoelectron spectroscopy) measurements were performed on X-ray photoelectron spectroscopy (K-Alpha+, Thermo Fisher technology). Inductively coupled plasma spectroscopy (ICP) analysis was conducted on an Ultima2 spectrometer. Thermogravimetric analyses (TGA) were carried out on a Mettler Toledo TGA/SDTA 851^e analyzer under an N_2-flow atmosphere with a heating rate of 5 °C·min^{-1} in the temperature range of 30−800 °C. The TEM samples were prepared by drop-casting the sample suspension onto a carbon-coated Cu TEM grid. HAADF-STEM images and EELS measurements of samples were recorded by JEOL JEM F200 transmission electron microscope (operated at 200 kV) using a Gatan imaging filter system (Gatan 1077 module) at an energy resolution of about 1 eV. Solid-state NMR spectra were acquired on a Bruker AVANCE III HD 500 MHz spectrometer equipped with an Ultra Shield Plus magnet (11.7 T) and a MAS VTN probe for solid-state experiments. The ICP-OES measurements were performed using an Agilent 720 EX spectrometer. The instrument, equipped with a 40 MHz air-cooled RF generator and an axial-view configuration, features a full-range optical system (167-785 nm) that simultaneously captures the entire spectrum via a charge-coupled device (CCD) detector employing I-MAP image mapping technology. The DC chemiresistive sensors were developed by drop-casting the acetonitrile suspension of sample onto the silver interdigital electrodes. A mixture of POM sample (50 mg) and acetonitrile (100 μL) was stirred and grind for 10 min at RT to obtain a well-dispersed suspension, then the sensor components were conveniently fabricated by drop coating the solution (20 μL) of POM material onto the interdigital electrodes (electrode width and gap: 0.20 mm), then dried at RT. The sensing performances were conducted by a homemade setup (Fig.S12), and the concentration of different gases in the analyte flow was controlled by a dynamic volumetric method and calibrated by a commercial instrument. Mass flow controllers (MFC, CS-200C, Beijing Sevenstar Qualiflow Electronic Equipment Manufacturing Co., Ltd., China) were utilized to control the flow of gas, MFC1 for bubbling gas (dry air for bubbling into the water), MFC2 for mixed gas (mixing with dry air and analyte gas), and MFC3 for dry air (blank measurement), MFC4 for analyte gas (analyte gas is mixed with dry air).

S1.2 Synthesis of 1a.

A mixture of $K_7HNb_6O_{19}\cdot 13H_2O$ (0.30 g, 0.219 mmol), K_3PO_4 (0.05 g, 0.236 mmol), Na_2TeO_3 (0.08g, 0.036 mmol) and 1 mL CH_3CN was mixed in 6 mL deionized water. After magnetic stirring for half an hour, $AgNO_3$ (0.04 g, 0.235 mmol) was added to this mixture, followed by one hour of magnetic stirring. The resulting mixture was sealed in a glass bottle (23 mL) and heated at 80 ℃ for 4 days. After cooling to room temperature, white crystals were obtained. Yield: 60 mg (14.2%, based on Nb). ICP analysis (based on dried sample) calculated (found %) for $H_{13}K_6Na_{13}[(Te_4Nb_9O_{36})_4Ag_6Te_2Nb_2O_6]\cdot 35H_2O$ (**1**): Na, 2.97 (3.11); K, 2.33 (2.24); Ag, 6.44 (6.77); Nb, 35.12 (37.51); Te, 22.85 (21.14). On the basis of the synthesis of **1a**, 0.05g of boric acid was added to obtain white block-shaped crystals **1b**.

Table S1. Crystal data of **1a.**

Compound	1a
Empirical formula	$Ag_6K_6Na_{13}Nb_{38}O_{185}Te_{18}$
Formula weight	9968.07
Crystal system	orthorhombic
Space group	*Pnma*
a (Å)	36.229(4)
b (Å)	32.370(3)
c (Å)	19.0896(18)
α (°)	90
β (°)	90
γ (°)	90
V (Å^3)	22387(4)
Z	4
F (000)	18052.0
ρ_{calc} (g/cm^{-3})	2.958
Temperature (K)	150
μ (mm^{-1})	4.914
Reflection collected	85322
Independent reflections	20064[R_{int}=0.0312, R_{sigma}=0.0282]
Data / restraints / parameters	20064/24/1240
GOF on F^2	1.030
Final R indices [I= 2σ(I)]	R_1=0.0506, wR_2=0.1375
R indices (all data)	R_1=0.0586, wR_2=0.1407
SQUEEZE Details	
Solvent accessible volume / Å^3	4266.6
Electrons per unit cell	1721

$R_1=\sum||F_o|-|F_c||/\sum|F_o|$; $wR_2=[\sum w(F_o^2-F_c^2)^2/\sum w(F_o^2)^2]^{1/2}$; $w=1/[\sigma^2(F_o^2)+(xP)^2+yP]$, $P=(F_o^2+2F_c^2)/3$, where x=0.0748, y=660.5496

Crystals were collected on a Bruker APEX III CCD area diffractometer equipped with a fine focus, 2.0 kW sealed tube X-ray source (Mo Kα radiation, λ = 0.71073 Å) operating at 150 K. The empirical absorption correction was based on equivalent reflections. Structures were solved by direct methods followed by successive difference Fourier methods. Computations were performed using SHELXTL and final full-matrix refinements were against F^2. The contribution of disordered solvent molecules to the overall intensity data of structures was treated using the SQUEEZE method in PLATON. The crystal data of **1a** in Table S1. The CCDC 2450581 contains the crystallographic data for these compounds.

Table S2. Comparison table of parameters **1a** and **1b.**

parameters		1a	1b
Crystallographic data	Crystal system	orthorhombic	orthorhombic
	Space group	*Pnma*	*Pnma*
	a (Å)	36.229(4)	36.130(5)
	b (Å)	32.370(3)	32.215(5)
	c (Å)	19.0896(18)	19.117(3)
	α (°)	90	90
	β (°)	90	90
	γ (°)	90	90
	V (Å^3)	22387(4)	22251(6)
Ag···Ag distances		3.300-3.410 Å	3.292-3.379 Å
τ_{ave}(298K)		Countless	146.26 us
k_{nr}		10^8 s^{-1}	6.8×10^3 s^{-1}
quantum yield		< 0.1%	1.1%
BO_3/BO_4 ratios		0	98.5/1.5
B wt% from ICP		0	0.5wt%

Section S2 Structures and Characterizations

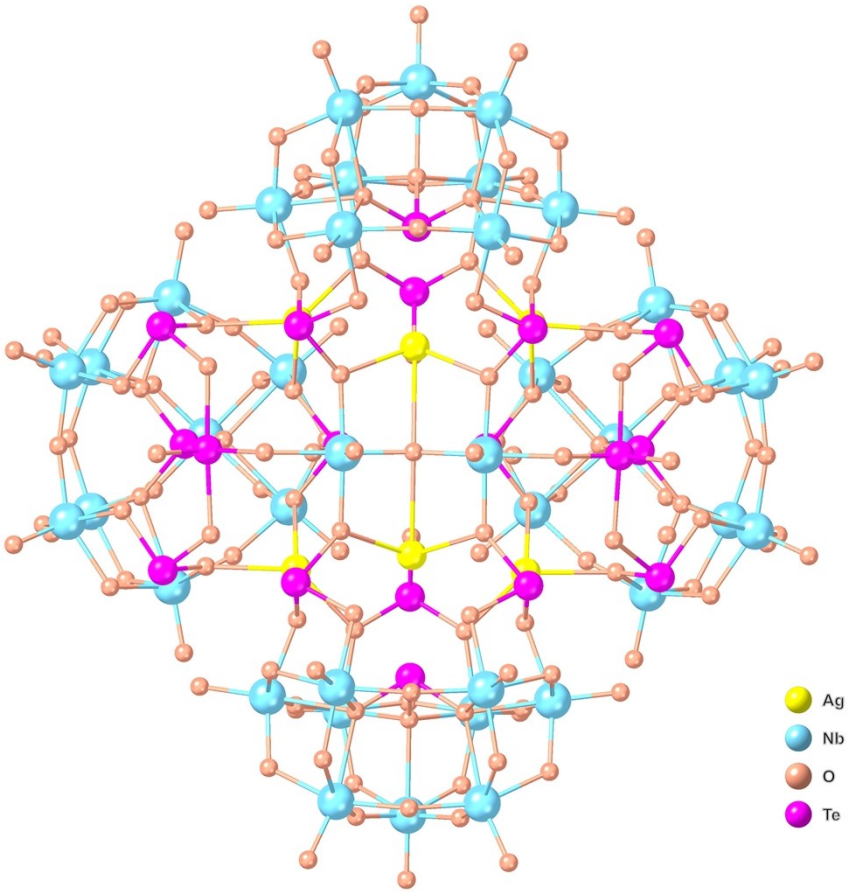

Figure S1 View of the ball-and-stick representation of compound **1a**.

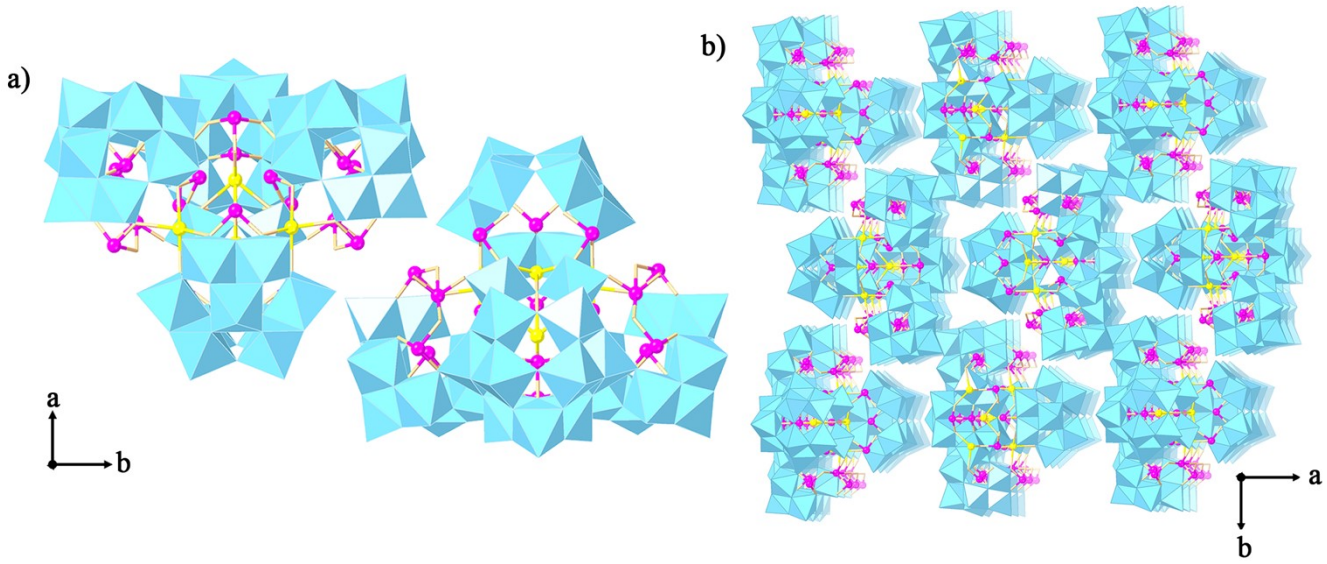

Fig. S2 a) Schematic diagram of "head to head" arrangement; b) Three-dimensional stacking diagram of compound **1a** along the *c* axes.

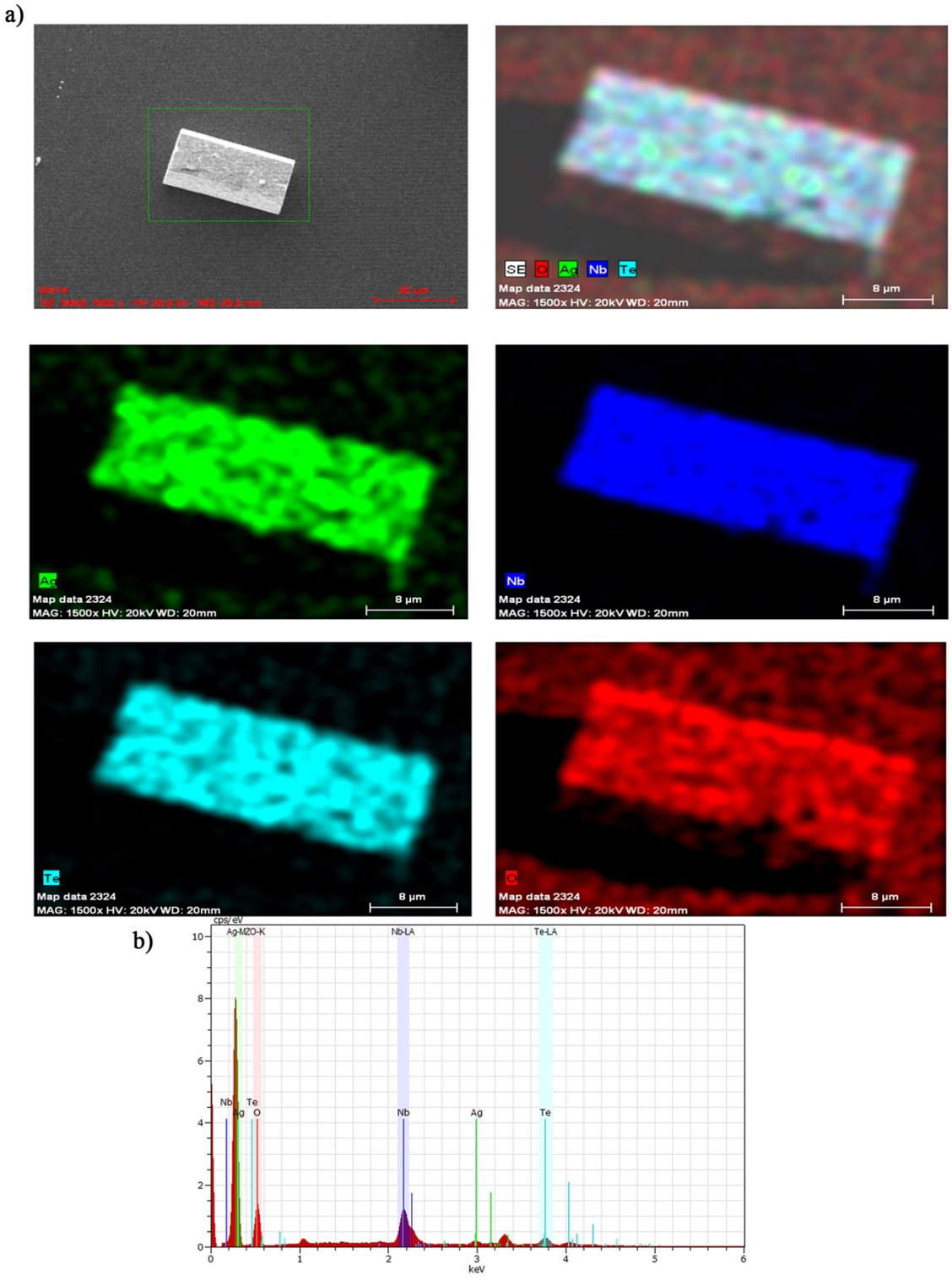

Fig. S3 a) b) SEM image and EDS elemental mapping of **1a**.

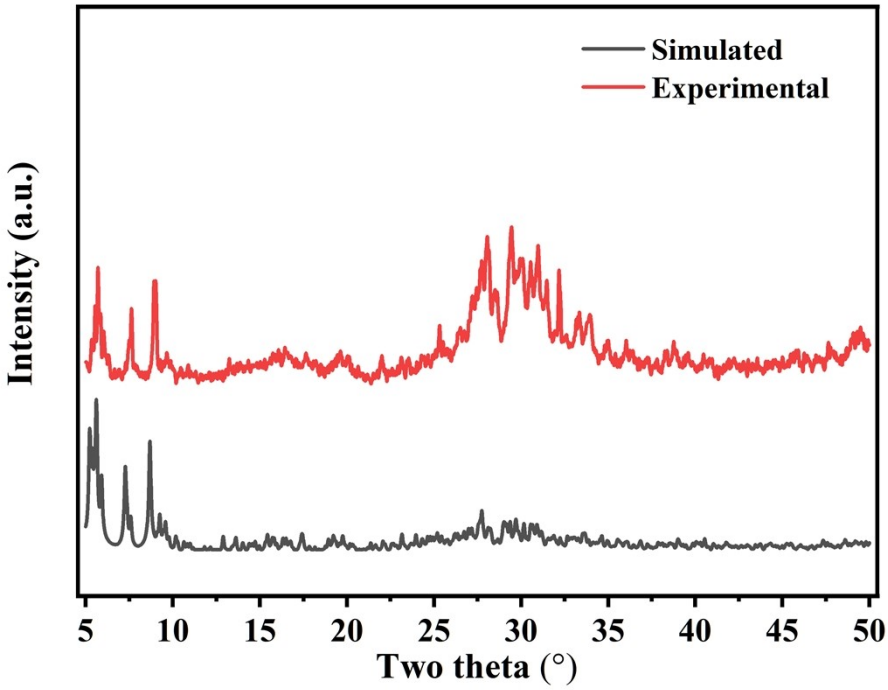

Fig. S4 The PXRD pattern of **1a**.

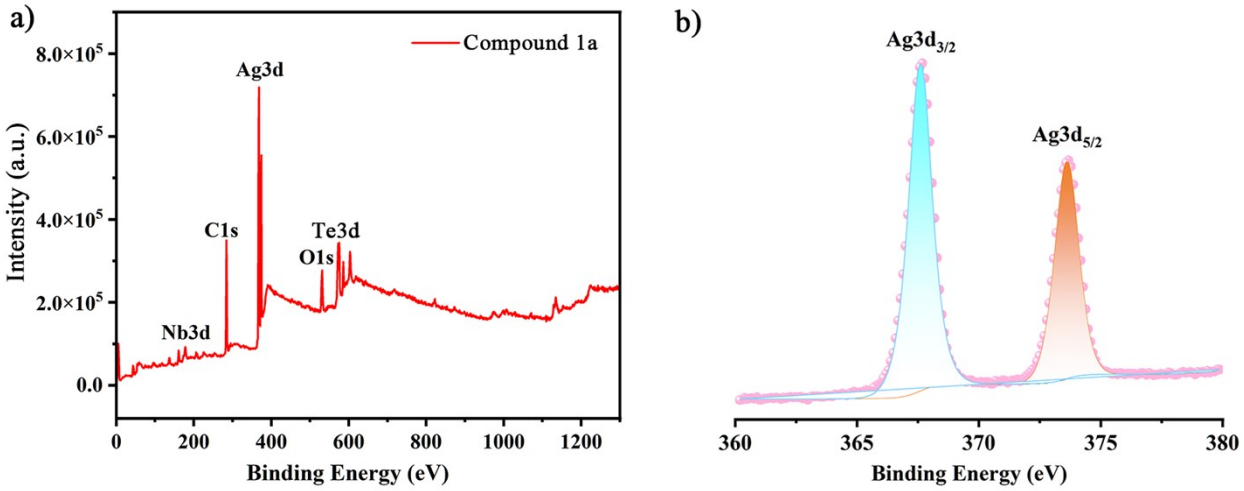

Fig. S5 a) XPS spectrum of **1a**; b) High resolution XPS spectrum of Ag $3d_{3/2}$,$3d_{5/2}$ of **1a**.

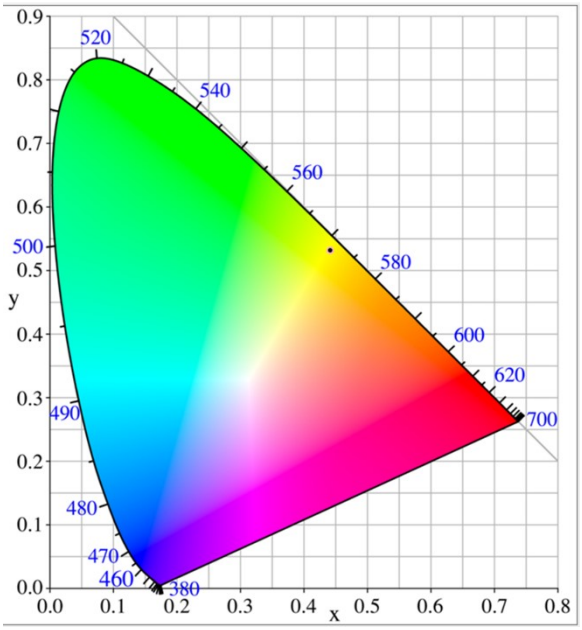

Fig. S6 The CIE standard colorimetric system corresponding to the emission spectra of **1b.**

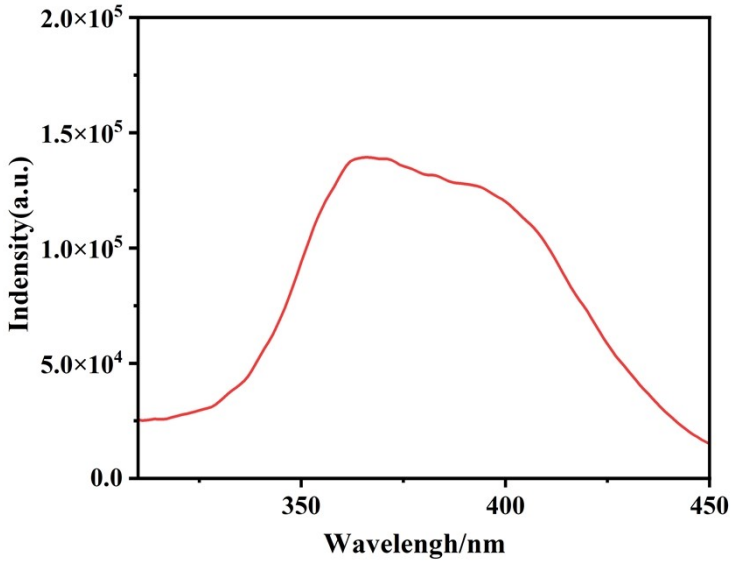

Fig. S7 The excitation wavelength optical image of **1b**.

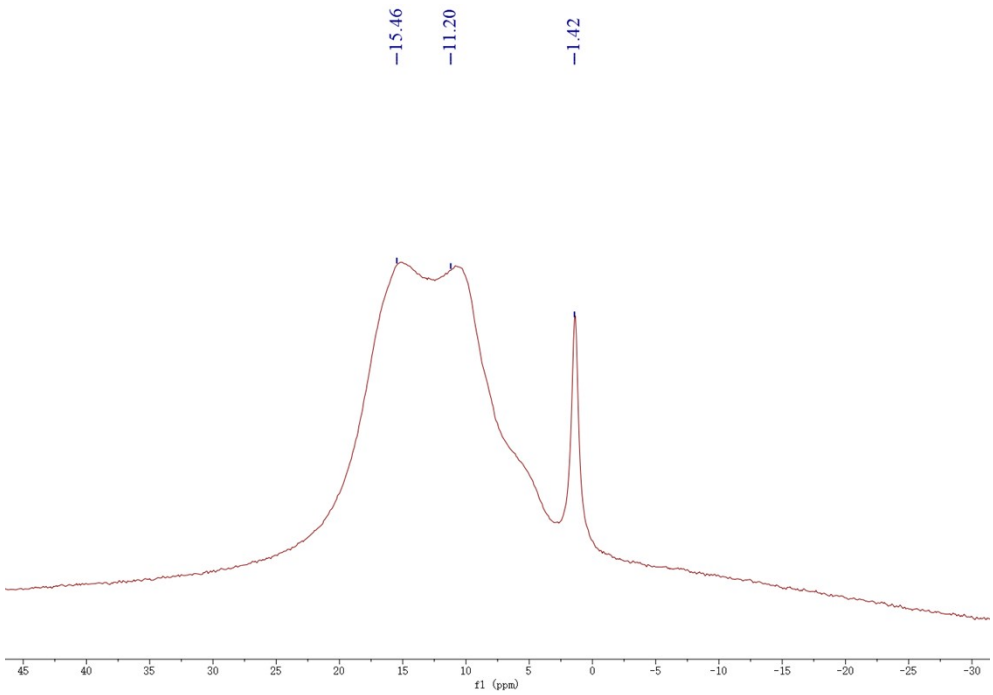

Fig. S8 Solid state nuclear magnetic resonance ^{11}B spectrum of compound **1b**.

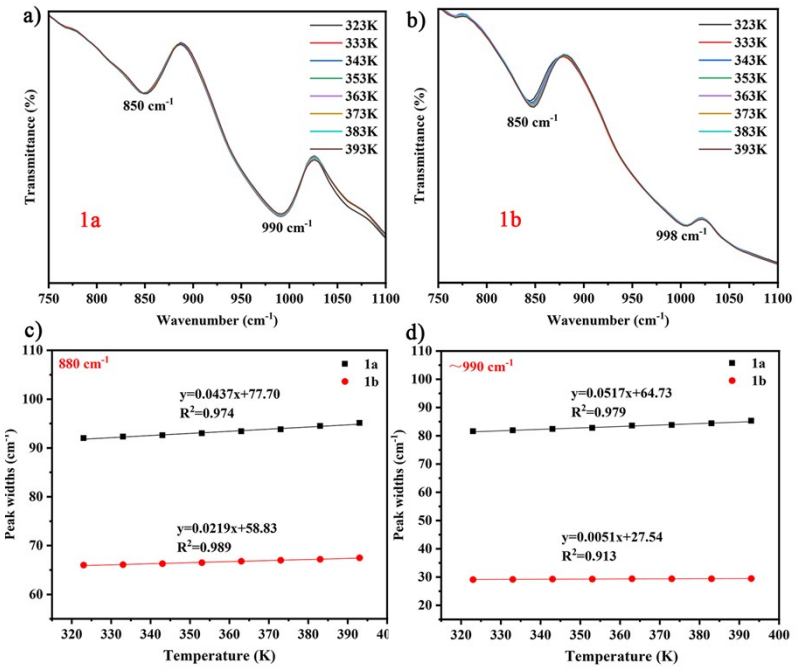

Fig.S9 a)-b) The variable-temperature infrared spectra of **1a** and **1b**. c)-d) Graphs of peak width variation with temperature near 880 cm^{-1} and 990 cm^{-1}. (We note that the uncertainty in this measurement is primarily limited by the instrumental resolution of 1 cm^{-1})

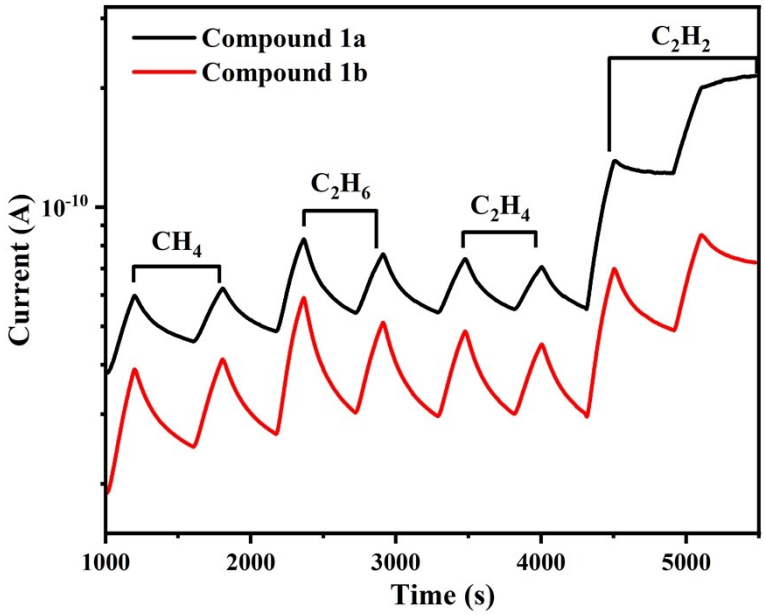

Fig. S10 Plot of the current response of compounds **1a** and **1b** to different gases.

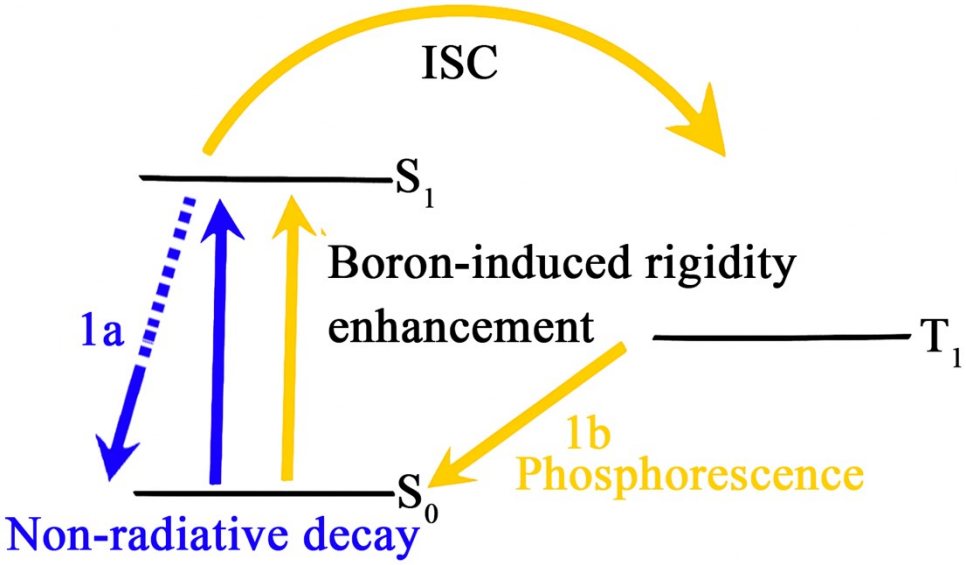

Fig. S11 Proposed mechanism for the boron-activated phosphorescence. Schematic diagram illustrating how boron-induced structural rigidity in **1b** suppresses non-radiative decay and enables triplet state phosphorescence, in contrast to the non-emissive compound **1a**.lot of the current response of compounds **1a** and **1b** to different gases.

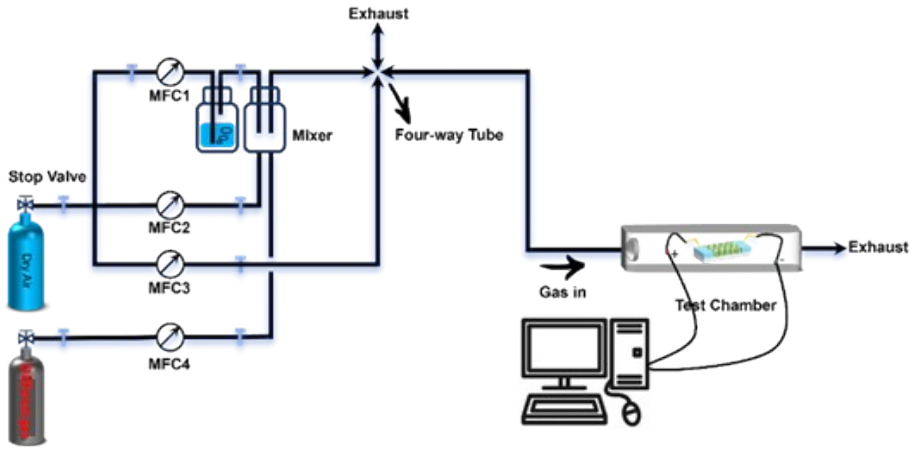

Fig. S12 Schematic diagram of homemade setup gas sensor

Section S3: References

1) Filowitz, M.; Ho, R. K. C.; Klemperer, W. G.; Shum, W. *Inorganic Chemistry* **1979**, 18 (1), 93-103.